



ELSEVIER

Journal of Nuclear Materials 271&272 (1999) 290–295

Journal of
nuclear
materials

www.elsevier.nl/locate/jnucmat

Microstructural evolution and radiation stability of steels and alloys

V.N. Voyevodin^{*}, I.M. Neklyudov, V.V. Bryk, O.V. Borodin

NSC 'KIPT', 310108 Kharkov, Ukraine

Abstract

Results of a systematic investigation of structure–phase transformations in the main FSU (Former Soviet Union) construction steels and alloys of ferritic and austenitic classes irradiated in reactors and in heavy ion accelerators are presented. Features in the dislocation structure evolution for these steels related to differences in stacking fault energy are considered and the role of cold deformation in swelling behaviour is investigated. The mechanisms of infiltration and compulsory alloying of second phase precipitates during irradiation as a result of mutual recombination at structural defects in interphase boundaries are discussed. The role of second phase formation and evolution on swelling behavior processes is investigated. The influence of undersized and oversized alloying elements (B, Si, Ti, Nb, Mo, Sc) on different aspects of structure–phase transformations, which are generally defined as radiation stability over a wide interval of irradiation temperature and dose, is considered. © 1999 Published by Elsevier Science B.V. All rights reserved.

1. Introduction

Changes in the physical and mechanical properties of alloys and steels during irradiation with neutrons or charged particles are related to the evolution of the microstructure [1]. The work presented on radiation stability (swelling) of these materials is described from the point of view of the cooperative interaction of defects, structure elements, solid solution decomposition and the evolution of second phase particles.

2. Experimental procedures and materials

The following austenitic and ferritic–martensitic steels have been used as cladding and wrapper materials in fast breeder reactors and are suggested for use in fusion reactors. Chemical compositions of the steels investigated are presented in Table 1.

The microstructure of initial and irradiated steel specimens was examined with the aid of transmission

electron microscopes (TEMs): EM-125K TEM and JEM-100CX TEM equipped with ASID-4D adapter LINK Systems-860. A quantitative element analysis was carried out using the RTS-2/FLS program. Size and density of microstructural features were measured with automatic quantitative equipment.

For irradiation the ESUVI (material research heavy ion accelerator), the UTI (heavy ion accelerator), and fast reactors BOR-60 and BN-600 were used. Dose interval consisted 0.1–200 dpa for ion irradiation, maximum neutron fluence – 12.6×10^{26} ($E > 0.1$ MeV), corresponding to a dose level of 68 dpa, irradiation temperature 350–750°C.

3. Results and discussion

3.1. Evolution of dislocations structure

It has been recognised that there is a radical difference in the evolution of dislocation microstructure in fcc and bcc materials. That is important from the standpoint of radiation stability because the dislocation structure redistributes the fluxes of point defects and can influence the evolution of microstructure and composition [2].

^{*} Corresponding author. Fax: +38-572 351 703; e-mail: voyev@kipt.kharkov.ua

Table 1
Chemical compositions of the steels investigated

	Ni	Cr	Mn	Mo	C	Ti	Nb	Si	Sc	Treatment
Austenitic stainless steels, FCC lattice										
18Cr–10Ni	10.6	18.0	1.2	–	0.04	0.06	–	0.8	0.02–0.05	1050–1150°C, 20–30%/CW 0.5 h
16Cr–15Ni	14.5	15.5	0.8	2.9	0.04	–	0.8	0.3	0.05–0.2	1050–1150°C, 0.5 h, 20–30%/CW
13Cr–13Ni	13.2	13.1	2.5	0.5	–	2.7	–	–	0.05–0.2	1050–1150°C, 0.5 h, 20–30%/CW
16Cr–11Ni	10.7	16.2	1.3	2.3	0.06	–	–	0.6	–	1050–1150°C, 0.5 h, 20–30%/CW
ChS–68	14.8	15.45	1.29	2.37	0.06	0.38	–	0.44	B 0.02	1050–1150°C, 0.5 h, 20–30%/CW
EP–172	14.4	15.2	0.42	2.66	0.08	–	0.64	0.12	B 0.01	1050–1150°C, 0.5 h, 20–30%/CW
EI–847	14.5	15.5	0.8	2.9	0.04	–	0.8	0.3	–	1050–1150°C, 0.5 h, 20–30%/CW
Ferritic–martensitic stainless steels, BCC lattice										
13Cr–2Mo	0.2	12.1	0.5	1.8	0.15	–	0.25	0.5	–	–
9Cr–2MoI	–	9.42	0.7	1.5	0.13	–	0.31	0.6	–	–
EP–450	0.2	12.1	0.5	1.8	0.15	–	0.25	0.5	–	–

Fcc materials (Ni, high nickel alloys, austenitic steels) follow a traditional evolution scheme with increasing dose: interstitial clusters → Frank loops $a/3\langle 111 \rangle$ → perfect loops $a/2\langle 110 \rangle$ → dislocation network.

It is necessary to pay attention to high sensitivity of transformation stage from Frank loops to perfect loops as a function of stacking fault energy. Alloy composition can influence the stacking fault energy and the energetic characteristics of point defects which in turn can change the evolution of the dislocation structure. Another important feature in deformed steels is the nonuniform dislocation distribution on grain boundaries, and the formation of ‘cell’ structure. Dislocation densities in cell boundaries can be an order of magnitude higher than inside cells, and their evolution must be taken into account.

Local difference in cold work deformation will lead to local nonuniformity in dislocation distribution during irradiation. Comparison of the dislocation structure in materials after different treatments is shown in Table 2.

In cold worked specimens the loops size slightly decreased in comparison with annealed material. The relative concentration of faulted and perfect loops shifted to increasing concentrations of faulted loops. The defect structures of $\text{Cr}_{16}\text{Ni}_{11}\text{Mo}_3$ and $\text{Cr}_{18}\text{Ni}_{10}$ steels show some variation in size and concentration of dislocation loops compared with steel $\text{Cr}_{16}\text{Ni}_{15}\text{M}_3\text{Nb}$, but the general tendency does not change. These results allow some deductions be made about close interlink between chemical composition of irradiated materials with behaviour of the dislocation structure. This behaviour is defined not by the nominal composition and alloying of materials but mainly by the content of impurities in solid solution resulting from the thermal and radiation exposure. From this point of view there is a marked difference in dislocation loop behaviour in a steel after different thermal treatments.

The formation of dislocations with the energetically nonfavourable Burgers vector $a\langle 1\ 0\ 0 \rangle$ is the main feature of dislocation behaviour in irradiated ferritic steels. Dislocation structure development in irradiated ferritic–martensitic steels are quite different in the two phases: ferrite and tempered martensite. This difference can be defined by the initial dislocation density which is two orders higher in tempered martensite than in ferrite and by the different interstitial content, mainly carbon [3].

In ferrite, the initial dislocation density exert only a slight influence on the formation of a radiation-induced network at doses higher than 20 dpa. The microstructure evolves accordingly with the scheme (collapsed vacancy clusters + interstitial clusters → interstitial loops).

In tempered martensite the situation is different and the microstructural evolution is, (initial dislocation network → collapsed vacancy clusters + interstitial clusters → cluster interaction with initial dislocations or

Table 2

Structural parameters of both dislocation and voids in austenitic stainless steels irradiate with chromium ions ($E = 3$ MeV, $D = 2$ dpa, $T = 600^\circ\text{C}$)

Materials	T_{irr} ($^\circ\text{C}$)	Average diameter of loops (nm)	Density of loops (cm^{-3})	Number of interstitials (cm^{-3})	Average diameter of voids (nm)	Voids density (cm^{-3})	Vacancy number in voids (cm^{-3})
$\text{Cr}_{16}\text{Ni}_{15}\text{Mo}_3\text{Nb}$	650	34.5	2.2×10^{15}	4.3×10^{19}	2.0	6×10^{14}	1.2×10^{17}
	700	81.0	1.3×10^{15}	9.2×10^{19}			
$\text{Cr}_{16}\text{Ni}_{15}\text{Mo}_3\text{Nb}20\%\text{CW}$	650	30.5	1.5×10^{15}	2.5×10^{19}	12.0	4×10^{14}	2.0×10^{19}
	700	69.0	1.1×10^{15}	7.2×10^{19}			
$\text{Cr}_{16}\text{Ni}_{15}\text{Mo}_3\text{Nb} + 800^\circ\text{C}$, 200 h	650	25.0	2.0×10^{15}	1.1×10^{19}	7.0	6×10^{14}	5.4×10^{19}
$\text{Cr}_{18}\text{Ni}_{10}\text{Ti}$	650	32.0	3.3×10^{15}	3.7×10^{19}			
$\text{Cr}_{16}\text{Ni}_{11}\text{Mo}_3$	650	41.5	1.2×10^{15}	2.4×10^{19}			

transformation into interstitial loops \rightarrow loops growth and interaction \rightarrow network formation).

In such a way ferrite and tempered martensite form different dislocation networks during irradiation that subsequently define the degree of interaction of dislocations and vacancy voids.

The practically important result of loop coalescence through glide and climb is the formation of stable dislocation network at comparatively low homologous temperatures ($\sim 0.2 T_m$ K) compared to fcc's, where dislocations are less mobile, and dislocation networks form at temperatures of $(0.35\text{--}0.45 T_m)$. Compared to fcc's the network, dislocation density for ferritic steels for irradiation to doses of 30 dpa ($\rho_d = 3.5 \times 10^9 \text{ cm}^{-2}$) is less than the value of $10^{10}\text{--}10^{11} \text{ cm}^{-2}$ usually observed in austenitic steels. As a consequence of the low dislocation density, the sink capacity in ferritic alloys is considerably lower than in austenitic steels at identical irradiation conditions.

From the point of view of void swelling, the phase condition of the material during irradiation defines the dynamic balance of point defects which escape recombination and correspondingly, the distribution of void parameters, and the magnitude of swelling.

The dislocation structure component exerts a very important influence on void swelling behaviour. This is seen by comparing the processes of nucleation and growth of voids in austenitic steels with different degree of cold deformation.

It is recognized that in austenitic steels void nucleation takes place mainly heterogeneously; at the same time, areas free from voids co-exist with areas where local swelling exceeds the swelling of steels in the annealed condition. With increasing deformation, the fraction of areas with low swelling increases, which leads to a decrease of average void swelling at the same irradiation parameters. Results of the present work show the effect of the initial dislocation structure on the formation and growth of voids. It is necessary to consider not only the total increase in sink capacity, but also to take into account the dislocation distribution, because

this will exert an influence on the bias factor. In a cold worked structure, the dislocation in cell boundaries, which survived during irradiation up to high doses, serve as neutral sinks.

It is very important to note that changes as a result of radiation-induced segregation (RIS) to the dislocation components of the matrix lead to changes in the main parameters, which define void swelling behaviour. These parameters are (a) – energetic and geometrical characteristics of point defects and their complexes; and (b) – concentration and capacity of point defect sinks.

It is known that the degree of microchemical evolution is defined by the mobility of point defects: that is why it is necessary to pay attention to this parameter.

The decrease in swelling at doses, which exceed the dose at which dislocation density in cold worked and annealed specimens are equalized, and some results on the swelling of steels with different chemical composition, that the influence of cold work is not limited to increasing point defect recombination. Changes in the dislocation structure and solute segregation during irradiation are also important.

Hindering of point defects flows with dislocation, and decreasing their concentration and mobility, reduces the rate of diffusive processes and retards segregation and correspondingly, phase formation. The microstructures of the steel $\text{Cr}_{16}\text{Ni}_{15}\text{Mo}_3\text{Nb}$ (solid solution treatment and 30%CW) show that cold work really reduces the rate of evolution of second phases enriched with nickel, and decreases the concentration of precipitates and their size.

Maintaining faulted loops up to high doses during irradiation of deformed steels serves to confirm the delaying of the depletion of the main alloying elements (Si, Mo, Nb) and Ni.

3.2. Evolution of second phase precipitates

The formation and evolution of second phase precipitates exert an influence on void swelling behavior

mainly as a result of changes due to RIS processes and changes in the morphology of precipitates [4].

In spite of the variety of experimental data described here, it is possible to identify a number of general features of phase evolution of multicomponent materials. In all cases, the behaviour of precipitates under irradiation depends on the structure of the precipitate–matrix interface and alters with the changing of precipitate–matrix conjugation (Fig. 1). After irradiation at a high dose, precipitates having a coherent interface or interfaces with low degree of incoherence are observed in the material. Such precipitates can exist in the initial specimens or can occur during irradiation. The higher stability of coherent precipitates is explained by the fact that a coherent interface has no defect sites and does not absorb point defects. Therefore, in the environment of the coherent precipitates located far from point defect sinks, segregation effects do not occur, i.e., the composition of the alloy does not change during irradiation. It means that the stability condition for coherent precipitates is not violated – thermally stable precipitates do not dissolve during irradiation. Under loss of coherence (in the process of precipitate growth), sinks for point defects develop at the precipitate–matrix interface (for example, misfit dislocations). Because of the interconnection between alloy component flux and point defect flux to precipitate–matrix interfaces (inverse Kirkendall effect) the growth rate of the incoherent precipitate changes. For binary alloys the condition of incoherent precipitate stability is formulated conveniently by introducing the notion of radiation-modified incoherent solubility. It is defined as the average solute concentration when the precipitate growth rate becomes equal to zero. Perhaps, the radiation-induced solubility depends on a degree of incoherence which is characterized by the sink strength of the precipitate–matrix interface. The

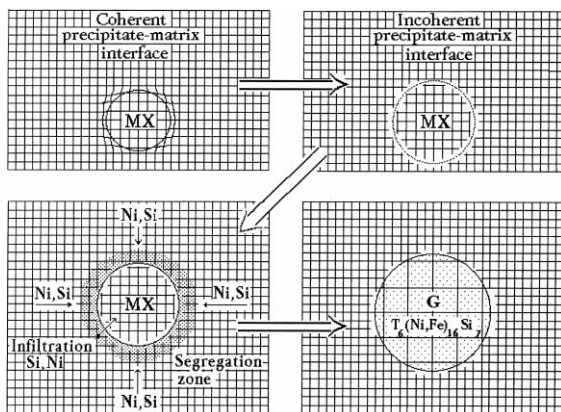


Fig. 1. Scheme of transformation MX-type precipitate during irradiations.

relation between thermal and radiation-induced solubilities depends on the relation between the diffusion coefficients of an alloy. In binary alloys segregation effects lead to either, dissolution of incoherent precipitates, or accelerated growth of them. This is true for coherent precipitates located near and at the point defect sinks as well.

The influence of precipitates on swelling behaviour is classified under three effects:

- direct, when accelerated recombination takes place
- indirect, when the general sink capacity of the system is changed
- intermediate, when the recombination rate of point defects changes in matrix due to changes of concentration of impurity elements.

The existence of second phase precipitates with a positive misfit, influences the behavior of vacancies and their complexes and a very close link exists between precipitate behaviour and void swelling.

MC precipitates have the biggest positive misfit (+19%) of all phases, due to lattice parameter mismatch [5]. A large positive misfit of precipitate to matrix induces vacancies flows, which stabilize growth during irradiation of MC–precipitate–vacancy complex.

Thus the formation of alternative vacancy sinks, that assists neutralisation of edge dislocations effectively reduces bias factor. Additionally low dispersed MC precipitates inhibit dislocations climb thereby leading leads to increasing level of recombination degree.

Mechanisms of impurity infiltration to noncoherent precipitates is shown on Fig. 2. It is known that noncoherency boundaries consist of regions of coherency

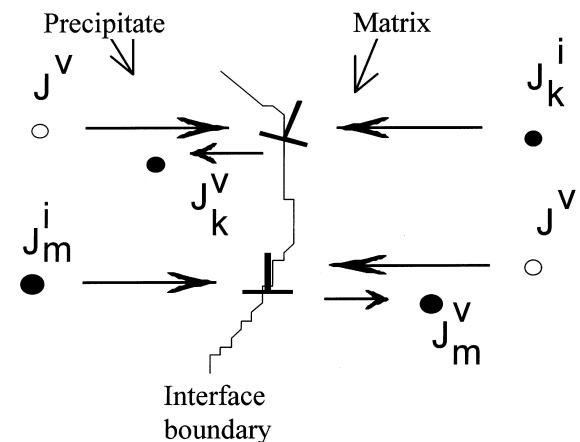


Fig. 2. Schematic picture of compulsory infiltration mechanism for elements segregated to non-coherent boundary, J^v – vacancy flow, $J_{k,m}^v$ – flow of atoms type k or m away from boundary on vacancies, $J_{k,m}^i$ – flow of atoms type k or m to boundary on interstitials.

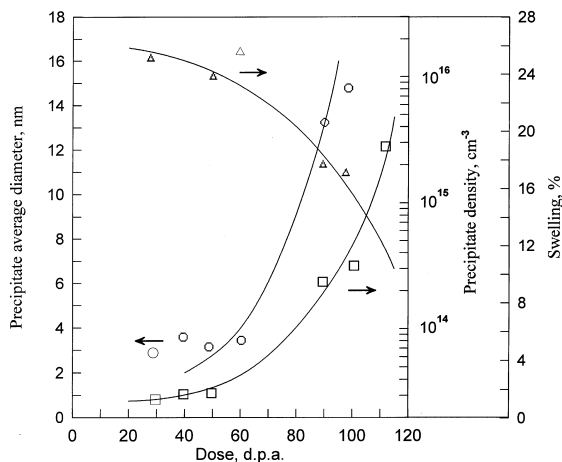


Fig. 3. Relationship between MC precipitate evolution and swelling for EI-847 steel (Cr^{3+} , $E = 3$ MeV, $T_{\text{irr}} = 650^\circ\text{C}$).

between matrix and phase and defected regions containing dislocations, point defects and others. RIS on the interface boundary occurs (see Fig. 3) due to the possibility that these defects areas absorb point defects [6]. Impurities, which migrated to a boundary via an interstitial mechanism and annihilate on dislocations, can migrate into a neighboring phase, if a vacancy arrives at this dislocation. According to this mechanism, injection of precipitate atoms into solid solution takes place. It is known that Ni is practically non-soluble in the carbides NbC and TiC, but as result of the mechanism described a compulsory alloying of these carbides with nickel takes place.

Very close link between the evolution of second phase precipitates and the dose dependence of swelling exist. It is recognized that increasing dose leads to a change in precipitate shape from spherical to globular and plate-like. It is significant that the moment of changing in precipitate form coincides with stationary stage of fast swelling (Fig. 4) [1]. The described modification of precipitate form means loss of coherency of MC precipitates. This rebuilding initiates a mechanism of phase evolution that leads to strong infiltration and accelerated growth of precipitates as a result of solute atoms flows from the matrix. Future rebuilding of globular precipitates to G-phase increases the rate of void growth.

3.3. Influence of alloying elements

Microimpurities of elements influenced swelling behaviour in accordance with their spatial distribution in the irradiated material. Theoretical and experimental investigations [1] to support the proposition that from physical point of view, the size factor of impurity is definite, its value depends on relation of atomic dimen-

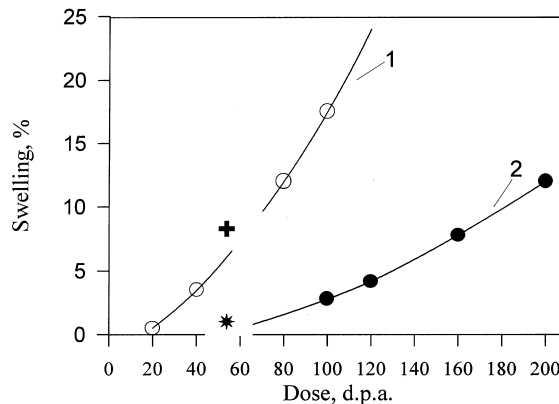


Fig. 4. Swelling of Sc bearing steels, 1 – EI-847 Cr^{3+} , 3 MeV, 2 – EI-847 + Sc, Cr^{3+} , 3 MeV, + – EI-847 BN-600, – EI-847 + Sc, BN-600.

sions for the impurity and the solid solution. The dilatation associated with the impurity defines its diffusion characteristics, the possibility of its participation in reactions with point defects and, therefore, in particular its segregation processes. Microalloying also changes stacking fault energy too.

The influence of microimpurities varies with metallic systems. In complex alloys and steels, several phenomena are realised simultaneously, and it is difficult to identify influence of specific impurity. Several features of steel EP-172 behaviour during irradiation, are connected to the addition of boron. Boron occupies a unique situation relative to α -iron. The atoms size ($R = 0.091$ – 0.097 nm) is too big for boron to occupy interstitial positions without large lattice dilatations. At the same time, it is too small for the formation of a substitutional solid solution. Due to the intermediate value of its atomic diameter, the formation of complex boron atom-vacancy (binding energy 0.4 eV) has an important role in the transport of boron atoms to structural defects in the crystal lattice, grain boundaries and interfacial boundaries. Boron has a big atomic radius relative to the interstitial elements: carbon and nitrogen, that suppress the diffusivity of the main alloying elements which are needed for formation of carbide and intermetallic phases. According with this α -solid solution of austenite contain biggest comparatively with nonboron steel concentration of such elements as Ni, Mo, Si, C, Nb. It is very important that the interaction of boron atoms with dislocations and dislocations loops changes the characteristics of dislocation structure evolution during irradiation [2]. Boron atoms form atmospheres around dislocation loops and reduce the stacking fault energy and the faulted Frank loop stage is extended. Maintaining a faulted loop stability delays the formation of a dislocation network (it is known that maximal swelling rate takes place when dislocation network is formed).

The improvement of radiation stability in steel Cs-68 compared to EI-847 and EP-172 is connected with more radical changes in its chemical composition, such as increasing the silicon concentration and the partial replacing of Nb with titanium.

The beneficial influence of silicon in swelling suppression is well known, but Si in austenitic steels serves as main segregant; that is why it is necessary to pay attention to the problems of phase stability. Ti has a few beneficial effects too, especially in combination with another alloying elements [7].

The authors have developed austenitic steels with small Sc (0.07–0.13 wt%) additions [8] with the purpose of increasing swelling-resistance.

The results of simulation and reactor investigations showed that the reductions of void swelling in modified steels is due essentially to increasing the incubation dose and slightly decreasing the swelling rate in the transition and steady state stages. The maximum effect due to reducing the size and concentrations of voids is achieved under a maximal saturation of solid solution with Sc or with a uniform distribution of small Sc-containing precipitates. Increasing the annealing temperature up to 1200°C leads to a further reducing of swelling due to increasing the Sc concentration in solid solution. The authors have suggested a few mechanisms of Sc influence on swelling behaviour [8] as follows:

- (a) big Sc atom ($R = 0.164$ nm) can form Sc–vacancies complexes with binding energy 0.6–0.8 eV and thus reduce vacancy concentrations;
- (b) Sc atoms can serve as a getter for gas atoms; difficulties in void nucleation under HVEM irradiation support this idea;
- (c) the formation of a stable system of small precipitates and an increase in phase stability;
- (d) big Sc-atoms form Cottrell atmospheres and stabilize the dislocation structure, which leads to increased recombination.

4. Conclusion

The radiation stability of investigated steels is defined by a cooperative interaction between elements of defect

structure, solid solution decomposition and second phase precipitation.

Difference in dislocation structure in materials with fcc and bcc metals plays an important rule in the radiation stability of these materials.

Dislocation structure exerts an influence not only on the preferential behaviour of point defects but changes the rate of radiation induced segregation. Solid solution decomposition due to RIS result changes matrix compositions and the shape and composition of second phase precipitates.

A mechanism of phase stability connected with coherence of interfacial boundaries is suggested. Alloying with under sized and oversized elements leads to essential changes in the evolution of structure and composition. The stability of the dislocation structure increases, point defect parameters and their concentrations are changed, and phase stability is modified. As a consequence of these phenomena mechanisms of swelling reduction can be developed.

References

- [1] V.N. Voyevodin, V.F. Zelenskij, I.M. Neklyudov, Effects of radiation on materials, ASTM 1046 (1) (1989) 193.
- [2] I.M. Neklyudov, V.N. Voyevodin, JNM 211–215 (1994) 39.
- [3] V.F. Zelenskij, I.M. Neklyudov, V.N. Voyevodin, Fizika i Himia Obrabotki Materialov 4 (1991) 5.
- [4] O.V. Borodin, V.V. Bryk, I.M. Meklyudov et al., Mater. Sci., Forum 97–99 (1992) 299.
- [5] E.H. Lee, P.J. Maziasz, A.F. Rowcliffe, in: J. Holland et al. (Ed.), Phase Stability During Irradiation, The Metallurgical Society of AIME, Warrendale, Pa, 1981, pp. 191–217.
- [6] O.V. Borodin, V.N. Voyevodin, I.M. Neklyudov, N.V. Kamushanchenko, Naychnue Vedomosti BGU 2 (5) (1997) 16.
- [7] O.V. Borodin, V.V. Bryk, V.N. Voyevodin, V.K. Shamarin, V.S. Neystroev, Effect of radiation on materials, 17th International Symposium, ASTM STP 1270, 1996, pp. 817–830.
- [8] V.F. Zelenskij, I.M. Neklyudov, Radiation materials science, Proceeding of the International Symposium on Radiation Materials Science, vol. 2, 1990, pp. 45–57.